Analytical Methods

DOI: 10.1002/ange.200501245

Interfacing Capillary Electrophoresis and Electrothermal Atomic Absorption Spectroscopy To Study Metal Speciation and Metal–Biomolecule Interactions**

Yan Li, Xiu-Ping Yan, and Yan Jiang*

Metallomics is a new field in the study of biometals and is related to genomics, proteomics, and metabolomics.[1] Trace metals in the environment may be adopted by biological systems to assist in the syntheses and metabolic functions of genes (DNA and RNA) and proteins. These metals may be beneficial or may pose a risk to humans and other life forms.[1–9] To establish metallomics as an integral biometal science, more robust and information-rich trace- and ultra-trace-chemical speciation analyses are needed for adequate risk or benefit assessments and to determine distributions of metals in humans, human blood serum, seawater, and even biological cells. Metal speciation is an important research subject in metallomics because the bioavailability and toxicity of metals on a molecular basis depends on their chemical state. Different species of the same metal be considered as essential, innocuous, or toxic.[1–9] Another important research subject in metallomics is the interaction between metal species and biomolecules, which is significant for biochemistry, biology, medicine, pharmacy, nutrition, agriculture, and environmental science.[1–9]

[*] Y. Li, Dr. X.-P. Yan, Y. Jiang
Key Laboratory of Functional Polymer Materials of the Ministry of Education of China
Research Center for Analytical Sciences
Department of Chemistry, Nankai University
Tianjin 300071 (China)
Fax: (+86) 22-2350-6075
E-mail: xpyan@nankai.edu.cn

[**] This work was supported by the National Basic Research Program of China (No. 2003CB415001), the National Natural Science Foundation of China (No. 20475028, 20437020), and the National Key Technologies R&D Program (2002A906A28-2).

Supporting information for this article is available on the WWW under http://www.angewandte.org or from the author.

Hybrid approaches are currently preferred for the study of metal speciation and metal–biomolecule interactions in numerous techniques developed to date.[6–9] The use of high-resolution separation methods in combination with highly sensitive detection techniques is necessary to improve the accuracy of the detection of metal speciation and metal–biomolecule interactions. The importance of capillary electrophoresis (CE) for such purposes has grown rapidly in the past decade, primarily as a result of its potential flexibility and easy implementation, high resolution, minimal sample and reagent consumption, and rapid and efficient separations with only minor disturbances of the existing equilibrium between the different species.[6,10–12] The use of inductively coupled plasma mass spectroscopy (ICP-MS) or optical emission spectroscopy (ICP-OES) as online detection techniques for CE promises substantial improvements in the sensitivity of the methods and in the identification and quantification of multispecies systems.[6]

Herein we report a new hybrid technique for nanoliter trace-metal speciation and metal–biomolecule interaction studies based on online coupling of CE to electrothermal atomic absorption spectroscopy (ETAAS). ETAAS provides high detection capability with low instrumental and operational costs. However, the discontinuous nature of ETAAS makes it troublesome when used in combination with continuous-flow systems and departs from the concept of monitoring continuously the chromatographic eluent.[13] We have developed a method for real-time ETAAS detection of the CE effluent by the direct interface of CE with ETAAS. The analysis was conducted on a laboratory-made thermospray interface, with no need for external heat sources or postcolumn derivatization steps. The features of this new hybrid technique are its simplicity, low instrument and running costs, easy operation, high sensitivity and selectivity, as well as its environmentally friendly nature.

The schematic setup of the CE–ETAAS hybrid system is shown in Figure 1. It includes a capillary electrophoresis system, a thermospray interface, and a graphite furnace. It is crucial for the interface to serve as a link that can harness the full potential of the separation method and the detector. ETAAS is sufficiently sensitive for speciation analysis, but graphite furnaces are not designed for continuous operation. Direct coupling of ETAAS to CE involves a number of problems because of the stepwise operational characteristic of the commercially available atomizers and because only a small volume can be injected into the furnace.

In view of above problems, a thermospray interface was designed to allow the real-time ETAAS monitoring of individual species separated by CE. A commercially available graphite tube and conventional ETAAS operating procedures were modified slightly to enable real-time detection of the CE effluent. First, the dosing hole of the graphite tube was enlarged to allow the tight attachment of a hollow graphite cap (1.0 mm i.d.), into which the thermospray vaporizer was inserted. The graphite cap behaved as a good heat-transfer medium for the vaporizer. A small gap was left between the vaporizer and the graphite capsule for carrier gas (argon) to flow through, thus enabling the delivery of the locally generated vapor into the graphite tube. Second, because the original dosing hole of the graphite tube was blocked by the thermospray interface, two more holes (1.0 mm i.d.) were made symmetrically beside the original dosing hole in the graphite tube to serve as hole for exhaust gas. The distance between the dosing hole and the hole for exhaust gas was 6.0 mm.

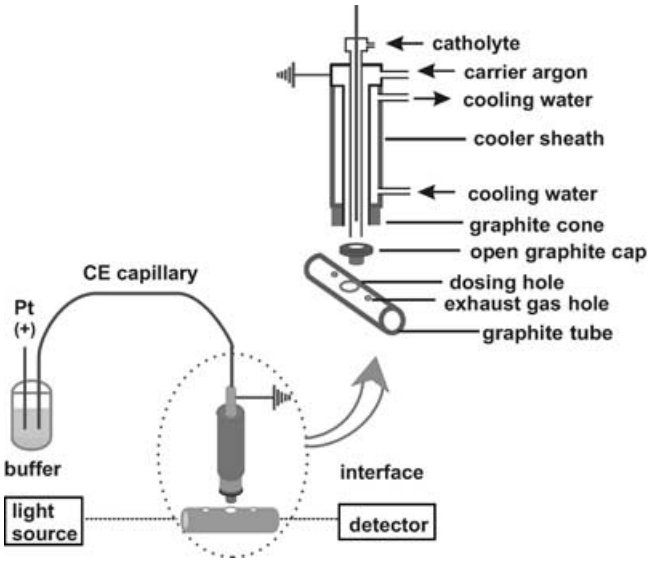

Figure 1. Schematic diagram for the new hybrid technique of capillary electrophoresis coupled online with electrothermal atomic absorption spectroscopy through a thermospray interface (not to scale).

To demonstrate the applicability of the developed hybrid technique for ultra-trace-element speciation, mercury and cadmium were chosen as target elements as they are highly dangerous metals, with an accumulative and persistent character in the environment. To ensure sufficient time for monitoring individual metal species in the CE effluent, the graphite furnace was programmed with seven successive thermostatic steps in the gas stop mode at an appropriate constant temperature for 99 s (the maximum time allowed) for each step. The temperature of the graphite furnace was set at 600 °C for the efficient atomization of mercury species. In this case, the lifetime of the graphite tube was 400 h. For cadmium speciation, the temperature of the graphite furnace was set at 1000 °C as a compromise between the lifetime of the graphite tube ($\approx$ 70 h) and the sensitivity of the method. The lifetime of the graphite tube decreased markedly when the temperature of the graphite furnace rose above 1200 °C.

In view of the complete introduction of CE effluent into the graphite tube, running electrolyte may influence the real-time ETAAS detection, depending on the nature of the element of interest. The goal herein was to achieve adequate resolution of the target species and to ensure subsequent detection without interference. Phosphate and borate buffers were suitable for mercury, but led to serious interferences for real-time ETAAS detection of cadmium at 1000 °C. Ammonium acetate (NH_4Ac) was preferred for cadmium speciation owing to its easy decomposition. As a running electrolyte with higher salt content causes undesirable blocking at the tip of the thermospray vaporizer after continuous heating for a long time, the concentration of the electrolyte should be as low as

possible, but should be enough to ensure good resolution and reproducibility for CE separation.

As shown in Figure 2A, three mercury species of methylmercury ($MeHg^{I}$), phenylmercury ($PhHg^{I}$), and inorganic mercury (Hg^{II}) were treated by baseline separation with CE in a 50 cm × 75 μm i.d. fused-silica capillary at 20 kV by using 15 mmol L^{-1} phosphate buffer at pH 6.8. The detection limit of the developed hybrid technique for mercury speciation was independent of mercury species. With an injection of 200 nL of sample solution in the hydrodynamic method, the detection limit ($S/N = 3$) of the mercury species was 14.8 ± 0.7 μg L^{-1} (as Hg). The developed method was validated by analyzing two certified reference materials GBW (E) 080393 (simulated natural water, National Research Center for Standard Materials, Beijing, China) and DORM-2 (dogfish muscle, NRCC, Ottawa, Canada). Both the quantified Hg^{II} content (97 ± 2 μg L^{-1}, $n = 5$) in GBW (E) 080393 and the methyl mercury content (4.28 ± 0.21 μg g^{-1}) in DORM-2 by using a simple external calibration method based on peak-area measurements are commensurate with the certified values (100 ± 4 μg L^{-1} for Hg^{II} in GBW (E) 080393, and 4.47 ± 0.32 μg g^{-1} for methylmercury in DORM-2).

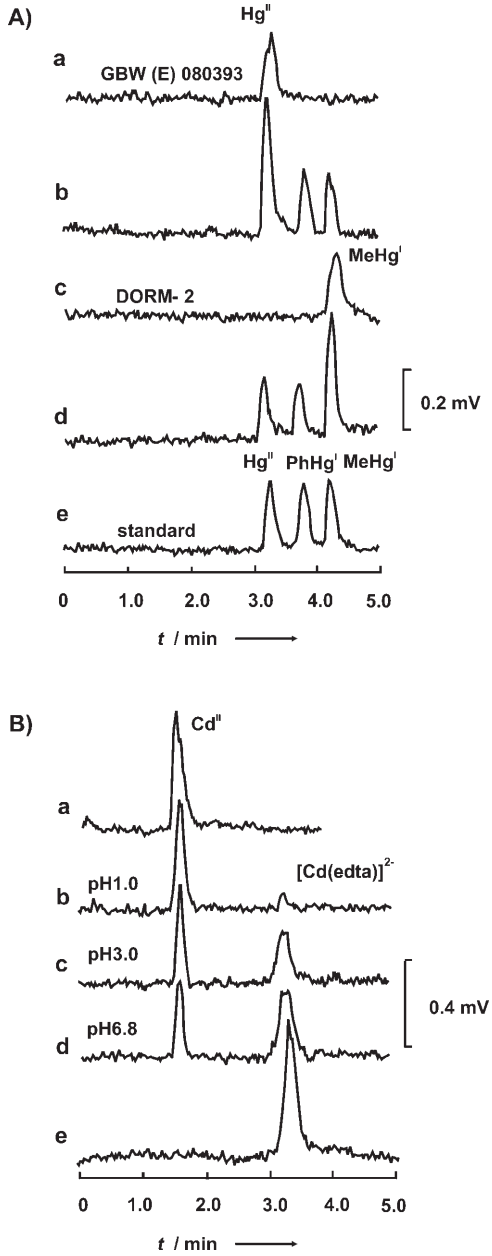

Figure 2. A) Electropherograms of a) GBW (E) 080393 (simulated natural water); b) GBW (E) 080393 spiked with of Hg^{II}, $PhHg^{I}$, and $MeHg^{I}$ (100 μg L^{-1} each); c) the extract of a certified reference material (DORM-2, dogfish muscle); d) the extract of DORM-2 spiked with of $MeHg^{I}$, $PhHg^{I}$, and Hg^{II} (100 μg L^{-1} each); e) a standard mixture of $MeHg^{I}$, $PhHg^{I}$, and Hg^{II} (100 μg L^{-1} each). B) Electropherograms of Cd^{II} and $[Cd(edta)]^{2-}$ for a) Cd^{II} (89 nmol L^{-1}), pH 6.8; b) a standard mixture of Cd^{II} (89 nmol L^{-1}) and EDTA (40 nmol L^{-1}), pH 1.0; c) a standard mixture of Cd^{II} (89 nmol L^{-1}) and EDTA (40 nmol L^{-1}), pH 3.0; d) a standard mixture of Cd^{II} (89 nmol L^{-1}) and EDTA (40 nmol L^{-1}), pH 6.8; e) a standard mixture of Cd^{II} (89 nmol L^{-1}) and EDTA (160 nmol L^{-1}), pH 6.8.

The developed hybrid technique was also applied to the study of the effect of the pH value on the reaction of Cd^{II} with disodium ethylenediaminetetraacetate (EDTA). As shown in Figure 2B, Cd^{II} and $[Cd(edta)]^{2-}$ were well separated by CE in a 50 cm × 75 μm i.d. fused-silica capillary at 20 kV when using NH_4Ac buffer (5 mmol L^{-1}) at pH 8.0. The peak area of Cd^{II} increased, whereas that of $[Cd(edta)]^{2-}$ decreased as the pH value decreased from 6.8 to 1.0 owing to the coalescence of H^+ with EDTA. The peak of Cd^{II} disappeared in the presence of excess EDTA at pH 6.8 (Figure 2Be).

The usefulness of the developed hybrid technique for the study of metal–biomolecule interactions was demonstrated by taking Cd^{II}/bovine serum albumin (BSA) and Hg^{II}/DNA as model systems. For this purpose, experiments were performed to obtain a series of incubation-time-dependent electropherograms of Cd^{II} and Cd–BSA adduct for a mixture solution of Cd^{II} (0.2 μmol L^{-1}) and BSA(0.1 μmol L^{-1}) (Figure 3A). Baseline separation of Cd^{II} and Cd–BSA adduct was carried out by CE in a 50 cm × 75 μm i.d. fused-silica capillary at 20 kV in the presence of 5 mmol L^{-1} of NH_4Ac-Tris buffer (pH 7.40) as running electrolyte. It was found from Figure 3A that about 55 % of the Cd^{II} was bound to BSA within 12 h and that the binding reaction between Cd^{II} and BSA reached equilibrium after 48 h. Hereafter no variations in the concentrations of Cd^{II} and Cd–BSA adduct were observed at various Cd^{II}/BSA molar ratios. The kinetics and binding constant for the interaction of Cd^{II} with BSA were evaluated from the time-dependent peak areas of Cd^{II} and Cd–BSA adduct. We assume that the interaction of Cd^{II} and BSA results in pseudo-first-order kinetic properties at the initial stage of incubation. The apparent kinetic rate constant (k) was then calculated by polynomial approximation of the concentration–time plots according to Equation (1).[14]

$$\ln \frac{C_{Cd}^{b}}{C_{Cd}^{0}} = -k\,t \qquad (1)$$

C_{Cd}^{0} and C_{Cd}^{b} are the initial molar concentration of Cd^{II} and the concentration of Cd–BSA adduct, respectively. The kinetic rate constant for the interaction of Cd^{II} and BSA was found to be independent of BSA concentration (zero-order kinetics for BSA). The value of k at various initial molar

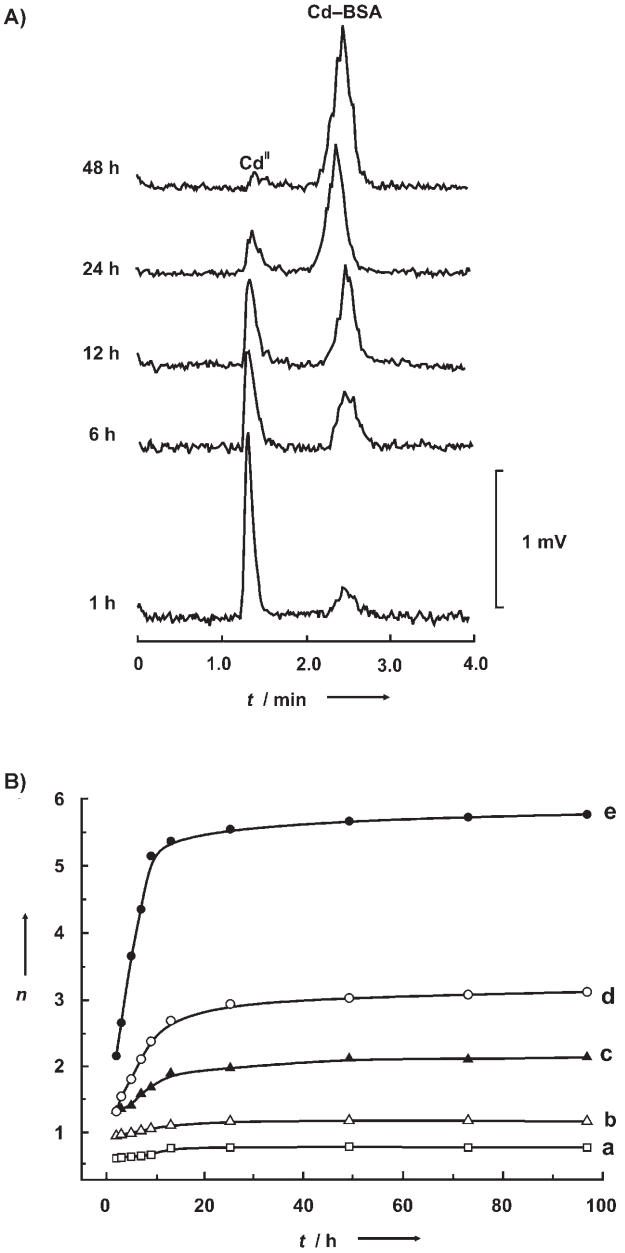

Figure 3. A) Incubation-time-dependent electropherograms of Cd^{II} and Cd–BSA adduct for the binding of Cd^{II} (0.2 μmol L^{-1}) with BSA (0.1 μmol L^{-1}). Baseline separation of Cd^{II} and Cd–BSA adduct was achieved by capillary electrophoresis in a fused-silica capillary (50 cm × 75 μm i.d.) at 20 kV by using NH_4Ac–Tris buffer (pH 7.40; 5 mmol L^{-1}) as running electrolyte. B) Number of cadmium atoms binding per BSA molecule at variable incubation time. Initial Cd^{II}/BSA molar ratio (initial Cd^{II} concentration of 0.2 μmol L^{-1}): a) 1:2; b) 1:1; c) 2:1; d) 4:1; e) 10:1.

ratios (0.5, 1, 2, 4, and 10) of Cd^{II}/BSA with an initial Cd^{II} concentration of 0.2 μmol L^{-1} at 37 °C was determined to be $(1.108 \pm 0.065) \times 10^{-3}$ min^{-1}.

The determination of Cd–BSA binding constant (K_b) was based on the bimolecular reaction between the donor (Cd^{II}) and the acceptor (BSA). If the concentration of BSA was kept constant, but different concentrations of Cd^{II} were added in the mixture, the value of K_b could be estimated by using a linear regression of a Scatchard plot.[15] based on the following expression [Eq. (2)]:

$$\frac{C^{b}_{Cd}}{C^{f}_{Cd}} = -K_b C^{b}_{Cd} + C_{BSA} K_b \quad (2)$$

In Equation (2), C^{b}_{Cd} and C^{f}_{Cd} are the concentrations of bound Cd^{II} (i.e. Cd–BSA adduct) and Cd^{II}, and C_{BSA} is the concentration of the binding site on the BSA. The number of Cd atoms bound per BSA molecule (n) was calculated from the change in the peak areas of Cd^{II} and Cd–BSA adduct based on Equation (3):[14]

$$n = \frac{C^{0}_{Cd}}{C^{0}_{BSA}} \frac{S^{b}_{Cd}}{S^{f}_{Cd} + S^{b}_{Cd}} \quad (3)$$

In Equation (3), C^{0}_{Cd} and C^{0}_{BSA} are the initial concentrations of Cd^{II} and BSA, respectively, S^{f}_{Cd} and S^{b}_{Cd} are the peak areas of Cd^{II} and Cd–BSA adduct, respectively. As such, the binding constant of Cd^{II} with BSA was estimated to be 2.68×10^7 L mol^{-1}, and the number of binding sites was 3.4 after incubation for 12 h. The evolution of Cd-BSA binding as a function of incubation time at various initial molar ratios of Cd^{II} to BSA is illustrated in Figure 3B. In the presence of excess Cd^{II}, the reaction proceeds more rapidly and the protein is attached to Cd to a higher degree, as expressed by a growing number of Cd^{II} bound per BSA molecule. The number of Cd atoms bound per BSA molecule increased more rapidly with higher molar ratios of Cd^{II} to BSA as the incubation time increased to 12 h. The number of Cd^{II} species bound per BSA molecule increased very slowly with increase of incubation time over a 12-h period. These results indicate that both strong and weak binding sites on the BSA molecule might contribute to the interaction of Cd^{II} with BSA in the presence of excess Cd^{II}. It was found that BSA binds up to 5 mol of Cd^{II} per mol of the protein when incubated with Cd^{II} in tenfold excess. The Cd^{II}/BSA stoichiometry ratio is greater than 3.4:1 and might be ascribed to the high affinity of soft Cd^{II} to some potential binding sites on BSA.

Representative electropherograms of the mixture of Hg^{II} and salmon sperm DNA are shown in Figure 4. Hg^{II} was well resolved from Hg–DNA adduct. The electropherograms show that Hg^{II} decreased, whereas the bound Hg–DNA increased with increasing concentration of DNA, as was clearly reflected by the variations in peak areas of Hg^{II} and the Hg–DNA adduct. The K_b value for the binding of Hg^{II} with DNA is 5.12×10^6 L mol^{-1}, and the number of binding sites is 0.2 for an initial DNA concentration of 2 mg L^{-1} (corresponding to a base-pair concentration of 3.4 μmol L^{-1}) after incubation with various concentrations of Hg^{II} for 1 h. Detailed studies are underway in our laboratory to determine the interactions of different mercury species with DNA, improve our understanding of the kinetic and thermodynamic properties, and to evaluate the relevant binding parameters, the damage of different mercury species to DNA, and the potential toxicity and environmental effects.

In summary, ETAAS was employed for the first time as a real-time CE detector. The combination of species separation by CE with direct ETAAS detection is suitable for elemental speciation. The technique could be used in investigations of

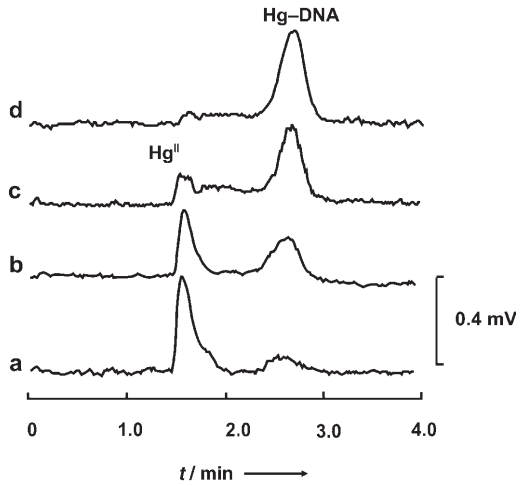

Figure 4. DNA-concentration-dependent electropherograms of Hg^{II} and Hg–DNA adduct for the binding of Hg^{II} (1 μmol L^{-1}) with DNA at various concentrations (μmol L^{-1}): a) 0.84; b) 1.7; c) 3.4; d) 6.8. Baseline separation of Hg^{II} and Hg–DNA adduct was achieved by capillary electrophoresis in a fused-silica capillary (50 cm × 75 μm i.d.) at 20 kV by using Tris–HAc buffer (pH 7.40; 50 mmol L^{-1}) as running electrolyte.

the thermodynamic equilibrium between the coexisting species and to determine the kinetics and stoichiometry of the binding reaction between metal species and biomolecules with good selectivity and high sensitivity.

Experimental Section

Certified reference materials DORM-2 (dogfish muscle; NRCC, Ottawa, Canada) and GBW (E) 080393 (simulated natural water; NRCSM, Beijing, China) were analyzed to check the accuracy of the developed hybrid technique for speciation analysis. An acid-leaching procedure was employed for extraction of mercury species from biological materials:[16] Briefly, hydrochloric acid (5 mL, 5 mol L^{-1}) was added to the certified reference material DORM-2 (0.3 g) in a 10-mL centrifuge tube. The mixture was then placed in an ambient ultrasonic bath for 10 min. After extraction, the suspension was centrifuged at 3500 rpm for 10 min, and the supernatant was transferred to a 10-mL flask. The supernatant was neutralized with NH_3H_2O and adjusted to pH 4.8–5.0 with phosphate buffer, then diluted to volume with doubly deionized water.

To simulate physiological conditions, NH_4Ac–Tris buffer (5 mmol L^{-1}) containing 100 mmol L^{-1} NaCl at pH 7.40 was used as the incubation solution. For the kinetic experiment, the reaction mixtures were incubated at 37 °C for more than 6 days, and aliquots were continuously taken from the same sample for analysis.

Received: April 9, 2005
Published online: September 15, 2005

Keywords: analytical methods · atomic absorption spectroscopy · electrophoresis · metal speciation · metallomics

[1] H. Haraguchi, *J. Anal. At. Spectrom.* **2004**, *19*, 5 – 14.
[2] C. Ash, R. Stone, *Science* **2003**, *300*, 925 – 925.
[3] L. A. Finney, T. V. O'Hallaoran, *Science* **2003**, *300*, 931 – 936.
[4] K. H. Thompson, C. Orvig, *Science* **2003**, *300*, 936 – 939.
[5] F. M. M. Morel, N. M. Price, *Science* **2003**, *300*, 944 – 947.
[6] *Comprehensive Analytical Chemistry, Vol. XXXIII Elemental Speciation* (Eds.: J. A. Caruso, K. L. Sutton, K. L. Ackley), Elsevier, Tokyo, **2000**, pp. 169 – 181.
[7] *Element Speciation in Bioinorganic Chemistry* (Ed.: S. Caroli), Wiley, New York, **1996**.
[8] *Chemical Speciation in the Environment* (Eds.: C. M. Davidson, A. M. Ure), Blackie Academic & Professional, London, **1995**.
[9] J. A. Caruso, M. Montes-Bayon, *Ecotoxicol. Environ. Saf.* **2003**, *56*, 148 – 463.
[10] S. Schäffer, P. Gareil, C. Dezael, D. Richard, *J. Chromatogr. A* **1996**, *740*, 151 – 157.
[11] E. Dabek-Zlotorzynska, E. P. C. Lai, A. R. Timerbaev, *Anal. Chim. Acta* **1998**, *359*, 1 – 26.
[12] X.-B. Yin, X.-P. Yan, Y. Jiang, X.-W. He, *Anal. Chem.* **2002**, *74*, 3720 – 3725.
[13] X.-H. Zhang, D. Chen, R. Marquardt, J. A. Koropchak, *Microchem. J.* **2000**, *66*, 17 – 53.
[14] A. R. Timerbaev, S. S. Aleksenko, K. Polec-Pawlak, R. Ruzik, O. Semenova, C. G. Hartinger, S. Oszwaldowski, M. Galanski, M. Jarosz, B. K. Keppler, *Electrophoresis* **2004**, *25*, 1988 – 1995.
[15] G. Scatchard, *Ann. N. Y. Acad. Sci.* **1949**, *51*,660 – 672.
[16] A. I. C. Ortiz, Y. M. Aibarrán, C. C. Rica, *J. Anal. At. Spectrom.* **2002**, *17*, 1595 – 1601.

